

# Lawrence Berkeley National Laboratory

## Recent Work

### Title

MOLECULAR BEAM PHOTOELECTRON SPECTROSCOPY OF SO<sub>2</sub>: GEOMETRY, SPECTROSCOPY, AND DYNAMICS OF SO<sub>2</sub><sup>+</sup>

### Permalink

<https://escholarship.org/uc/item/9mj496p3>

### Authors

Wang, L.  
Lee, Y.T.  
Shirley, D.A.

### Publication Date

1986-12-01

e.2



# Lawrence Berkeley Laboratory

UNIVERSITY OF CALIFORNIA

RECEIVED  
LAWRENCE  
BERKELEY LABORATORY

## Materials & Molecular Research Division

FEB 9 1987

LIBRARY AND  
DOCUMENTS SECTION

Submitted to Journal of Chemical Physics

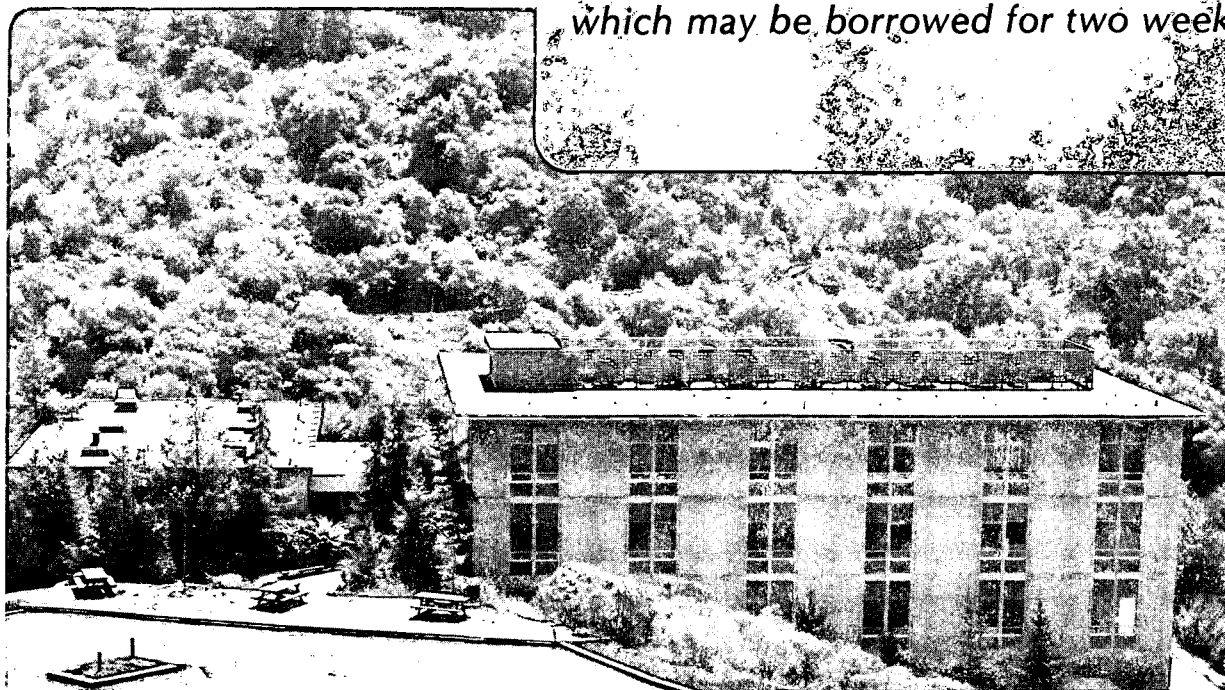
MOLECULAR BEAM PHOTOELECTRON SPECTROSCOPY OF  $\text{SO}_2$ :  
GEOMETRY, SPECTROSCOPY, AND DYNAMICS OF  $\text{SO}_2^+$

L. Wang, Y.T. Lee, and D.A. Shirley

December 1986

**TWO-WEEK LOAN COPY**

*This is a Library-Circulating Copy  
which may be borrowed for two weeks*



LBL-22413  
e.2

## **DISCLAIMER**

This document was prepared as an account of work sponsored by the United States Government. While this document is believed to contain correct information, neither the United States Government nor any agency thereof, nor the Regents of the University of California, nor any of their employees, makes any warranty, express or implied, or assumes any legal responsibility for the accuracy, completeness, or usefulness of any information, apparatus, product, or process disclosed, or represents that its use would not infringe privately owned rights. Reference herein to any specific commercial product, process, or service by its trade name, trademark, manufacturer, or otherwise, does not necessarily constitute or imply its endorsement, recommendation, or favoring by the United States Government or any agency thereof, or the Regents of the University of California. The views and opinions of authors expressed herein do not necessarily state or reflect those of the United States Government or any agency thereof or the Regents of the University of California.

LBL-22413

MOLECULAR BEAM PHOTOELECTRON SPECTROSCOPY OF  $\text{SO}_2$ :  
GEOMETRY, SPECTROSCOPY, AND DYNAMICS OF  $\text{SO}_2^+$

Laisheng Wang, Y.T. Lee, and D.A. Shirley

Materials and Molecular Research Division

Lawrence Berkeley Laboratory

and Department of Chemistry

University of California

Berkeley, California 94720

ABSTRACT

We have reinvestigated the HeI (584Å) photoelectron spectroscopy of SO<sub>2</sub> using a supersonic molecular beam. Improved resolution and rotational cooling allow us to observe new features and to resolve explicitly the vibrational structure in the first six electronic states, in the first three photoelectron bands. The adiabatic ionization potentials (IP's) were accurately determined for all six states. The  $\tilde{X}^2A_1$  ground state is assigned to the  $\nu_2$  mode exclusively. Irregularity of the vibrational progression on the high IP side was observed for the first time. A potential barrier (to linearity) is proposed to interpret the irregular vibrational spacings in the  $\nu_2$  vibration. The barrier height is estimated to be 0.42 eV (3400 cm<sup>-1</sup>). The complex second band contains two states. Abnormal vibrational structure in the  $\tilde{A}^2A_2$  state is explained by the principal excitation of the  $\nu_3$  mode. A potential barrier is present in the  $\nu_3$  potential surface, so that the ion has an asymmetric equilibrium geometry in this state. The barrier height is estimated to be less than 220 cm<sup>-1</sup>. A new progression is resolved in the  $\tilde{B}^2B_2$  state, which is assigned to be a combination of  $\nu_2$  with  $2\nu_3$ . The  $\nu_2$  vibration is observed to be strongly coupled with the  $\nu_3$  mode. The true adiabatic IP for the  $\tilde{C}^2B_2$  state is determined for the first time, as 15.902 ± 0.003 eV. The dynamics of the ion dissociation in this state is discussed and slow predissociations through the lower lying states are suggested. The  $\tilde{D}^2A_1$  and  $\tilde{E}^2B_1$  states are substantially broadened above the first few vibrational levels. Fast predissociations through the  $\tilde{C}^2B_2$  state are proposed to account for the spectral diffuseness. A weak band at about 14.6 eV, which had been assigned as a

configuration interaction (CI) satellite band, is found to be a HeI  $\beta$  line (537A) spectrum of the third band, due to the resolved vibrational structure. A true CI band at about 17.5 eV with resolved vibrational structure is observed. It consists of two  $\nu_1$  vibrational progressions, which look like two spin-orbit split components.

## I. INTRODUCTION

Many experimental methods have been used to study molecular ions, because of their important role in atmospheric chemistry and physics.<sup>1</sup> Molecular Photoelectron Spectroscopy (PES) is intrinsically concerned with the properties and spectroscopy of molecular ions, and PES has contributed a great deal to our knowledge of these ions. Although rotationally resolved PES is only possible for the lightest diatomic molecules with a conventional photon source (HeI, 584Å),<sup>2</sup> sufficiently high resolution PES can still provide substantial information about the energy levels, geometries, and dynamics of the molecular ions.<sup>3</sup> The nonresonant mechanism of the photoionization process provides access to many electronic states of a molecular ion.

Numerous investigations have been devoted to the  $\text{SO}_2^+$  ion, including electron impact,<sup>4</sup> Penning ionization,<sup>5</sup> absorption spectroscopy,<sup>6</sup> photoelectron spectroscopy,<sup>7-13</sup> photoelectron-photoion coincidence spectroscopy,<sup>14,15</sup> photoelectron-fluorescence coincidence spectroscopy,<sup>16</sup> and photoionization mass spectrometry.<sup>17-21</sup> Surprisingly, the high resolution photoelectron spectrum for this ion is still not available, and the spectroscopy of the ion in its various electronic states remains poorly understood. Even the molecular orbital order and the adiabatic ionization potentials in its different states are not completely consistent. In this paper, we report a high resolution HeI photoelectron spectrum of  $\text{SO}_2$  using supersonic molecular beams.

Sulfur dioxide in its ground state ( $X^1A_1$ ) is a bent molecule ( $\angle OSO = 119.3^\circ$ ), with  $C_{2v}$  symmetry.<sup>22</sup> There are seven valence molecular orbitals,<sup>23-26</sup> among which six are known to be accessible to HeI radiation (584Å).<sup>7-13</sup> The molecular orbital configuration can be represented as follows, with the bonding characters given underneath each orbital:<sup>23</sup>

$6a_1^2$	$2b_1^2$	$7a_1^2$	$4b_2^2$	$5b_2^2$	$1a_2^2$	$8a_1^2$
S 3s	S-O	S-O	weak	O-O $\sigma_u$	weak S-O	S
non-bonding	II bond	$\sigma$ bond	S-O bond	+ S-O	II bond	lone pair
				weak bond		

The  $8a_1$  orbital is mainly the sulfur lone pair, which is responsible for the bent geometry of the molecule. The  $1a_2$  and  $5b_2$  orbitals would be non-bonding based on only s and p orbitals, without considering the sulfur d orbitals. The  $6a_1$  orbital is the sulfur 3s lone pair, which is generally not accessible for electrostatic type electron analyzers with HeI (584Å) radiation. Therefore, photoionization by HeI can produce six electronic states of the molecular ion.<sup>7-13</sup> The assigned ordering of the states has not been totally consistent. The order given above is generally accepted.<sup>9</sup> However, for example, in a recent tabulation of HeI photoelectron spectra, Kimura et al. gave a different ordering, based on their ab initio assignment.<sup>12</sup>

The early HeI photoelectron spectrum of  $SO_2^+$  was taken by Turner et al.<sup>7</sup>, and by Eland and Danby.<sup>8</sup> Three bands were observed. One state was assigned to the first band, which corresponds to the ionization of the  $8a_1$  orbital. Two states were assigned to the second and third bands respectively, though Eland and Danby<sup>8</sup> pointed out that one single peak



at 16.67 eV was observed in the third band of their spectrum and proposed that it could arise from a third state in the band. Lloyd and Roberts<sup>9</sup> obtained a higher resolution spectrum of the third band and found that there were indeed three states in the band, which was in agreement with theoretical predictions.<sup>23-26</sup> Potts<sup>11</sup> obtained the low resolution HeI (584Å) and HeII (303.8Å) spectra of SeO<sub>2</sub> and SO<sub>2</sub>, trying to correlate the molecular orbitals in the two molecules. Recently, Holland, Parr, and Dehmer<sup>13</sup> measured the photoelectron asymmetry parameters and branching ratios for SO<sub>2</sub> in the 14-25 eV photon energy range by using synchrotron radiation.

The vibrational structure of the SO<sub>2</sub><sup>+</sup> PE spectrum is rather complicated, except for the first band, which was assigned to the  $\nu_2$  mode exclusively. In the second band, the state at higher IP was assigned to the  $\nu_2$  mode, but the state at lower IP was assigned in several ways; Turner et al.<sup>7</sup> assigned it by the  $\nu_2$  and  $\nu_3$  modes, while Eland and Danby<sup>8</sup> used the  $\nu_1$  and  $\nu_2$  modes. Cederbaum, Domcke, Niessen, and Kraemer<sup>27</sup> called the vibrational structure in this band "a difficult assignment problem" and performed an ab initio many-body calculation on the vibrational structures for the first two bands ( $\tilde{X}^2A_1$ ,  $\tilde{A}^2A_2$ , and  $\tilde{B}^2B_2$  states). The  $\tilde{X}$  and  $\tilde{B}$  states seemed to be well reproduced with the  $\nu_2$  mode only. They used the  $\nu_1$  and  $\nu_2$  modes to calculate the  $\tilde{A}^2A_2$  state. The result was less conclusive, because the experimental spectrum was not well resolved.<sup>7,8</sup> The third band of the spectrum is even more complicated, due both to the heavy overlapping of the last three states and to the band diffuseness.

A molecular beam photoionization study of  $\text{SO}_2$  was reported by Erickson and Ng.<sup>20</sup> They obtained the photoionization efficiency (PIE) curves for  $\text{SO}_2^+$ ,  $\text{SO}^+$ , and  $\text{S}^+$ . The first IP for  $\text{SO}_2$  was accurately determined to be  $12.348 \pm 0.002$  eV. The onsets for the photodissociative ionization processes  $\text{SO}_2 + h\nu \rightarrow \text{SO}^+ + \text{O} + e^-$  and  $\text{SO}_2 + h\nu \rightarrow \text{S}^+ + \text{O}_2 + e^-$  were measured to be  $15.953 \pm 0.010$  eV and  $16.228 \pm 0.030$  eV respectively. They observed a complicated PIE curve for  $\text{SO}_2^+$  in the 987-1006 Å range corresponding to the first band in the PE spectrum, from which they concluded that "the irregular spacing observed in the PIE curve rules out any simple assignment of the first photoelectron band to the  $\nu_2$  bending mode of  $\text{SO}_2^+$ ".

The relaxation of the  $\text{SO}_2^+$  ion has also been the topic of several research papers by different coincidence techniques.<sup>14-16</sup> An early photoelectron-photoion coincidence measurement showed that the dissociation of  $\text{SO}_2^+$  ion in the third band could not be explained by either a statistical model or a model of direct dissociation.<sup>14</sup> A threshold photoelectron-photoion coincidence study revealed that the  $\text{S}^+$  formation occurred only in a very narrow energy range above the threshold.<sup>15</sup> A photoion-fluorescence photon coincidence study of radiative and dissociative relaxation processes in VUV photoexcited  $\text{SO}_2$ <sup>16</sup> showed that emission from electronic states lying above the dissociation threshold could be observed; that is, the radiative decay was competitive with the nonradiative decay or dissociation.

Although there have been many experimental studies on the  $\text{SO}_2^+$  ion, few theoretical studies have been reported.<sup>23,27</sup> There has not been any

recent study. We hope that our high resolution PES study can spur more theoretical work on this ion.

In what follows, we will give in Sec. II a brief account of the experimental technique. The results will be presented in Sec. III. The discussion for the individual state and the summary will be given in Sec. IV and Sec. V respectively.

## II. EXPERIMENTAL

The molecular beam photoelectron spectrometer used for this study has been described in detail before.<sup>28</sup> Briefly, the supersonic SO<sub>2</sub> molecular beam was crossed perpendicularly by a photon beam from a rare gas discharge lamp. The electron energy analyzer consisted of a double electrostatic deflector operated at a pass energy of 1.0 eV, which sampled the photoelectrons at an angle of 90° with respect to both the photon beam and the molecular beam. The complete HeI (584Å) photoelectron spectrum of SO<sub>2</sub> (Matheson, Anhydrous Grade, 99.98%), expanded from 200 torr at room temperature through a 100 μm dia. nozzle and skimmed by a 0.9 mm dia. conical skimmer, was recorded with multichannel detection at a resolution of 13 meV FWHM, as measured on Ar<sup>+</sup> (<sup>2</sup>P<sub>3/2</sub>).

### III. RESULTS

The complete HeI photoelectron spectrum of  $\text{SO}_2$  is plotted in Fig. 1, with state labellings shown. The improved resolution and rotational cooling permit the vibrational structure in all the states to be explicitly resolved. Besides the three main bands, two other weak bands at about 14.6 and 17.5 eV are also observed, with resolved vibrational structure. They were assigned as two CI bands in a previous study.<sup>12</sup> An impurity peak of the  $\tilde{X} \text{N}_2^+$  ( $v=0$ ) is observable in the spectrum at 15.6 eV. The  $\tilde{B}^2\Pi_u$  state of  $\text{N}_2^+$  should be around 17.0 eV, but the intensity is negligible. Therefore, the  $\text{SO}_2^+$  spectrum is not affected. In Table I, the adiabatic IP's of the first six states of  $\text{SO}_2^+$  are given and compared with previous measurements where available, and the mean peak positions in all the states are listed in Tables II-VII. Our adiabatic IP for the ground state is in excellent agreement with the value obtained by Erickson and Ng.<sup>20</sup> We note that the first peak in the ground state does not represent the adiabatic IP. As already pointed out by Erickson and Ng, it is a hot band transition. This was confirmed by changing the  $\text{SO}_2$  stagnation pressure in the supersonic expansion. From Table II, it is seen that the interval ( $515 \pm 3 \text{ cm}^{-1}$ ) between the first and the second peak corresponds exactly to the fundamental  $\nu_2$  in the ground state  $\text{SO}_2$  ( $517.7 \text{ cm}^{-1}$ ).<sup>29</sup> It can be seen from Table I that all the previous PES determinations of the adiabatic IP were actually from the hot band. The onset of the third band represents another interesting situation, where the true adiabatic transition to the  $\tilde{C}^2B_2$  state is observed for the first time in the

current spectrum. All previous measurements failed to observe the first peak in this band. The adiabatic IP determined for the  $\tilde{C}^2B_2$  state in the present study is  $15.902 \pm 0.003$  eV. As shown in Table I, this value is considerably lower than the previously measured values.

The vibrational assignment and the discussion for the individual states are presented in the next Section.

#### IV. DISCUSSION

##### a. The First Band [ $\tilde{X}^2A_1(8a_1^{-1})$ state]

The separated spectrum of this band is shown in Fig. 2. The band contains only one state, which is formed by ionizing the outmost  $8a_1$  orbital of  $SO_2$ . The vibrational structure is completely resolved in Fig. 2. Erickson and Ng<sup>20</sup> observed a rather complicated structure in their PIE curve of  $SO_2^+$ , and concluded that it was impossible to make a simple assignment of this band in the PE spectrum to the  $\nu_2$  bending mode. However, the well-developed vibrational progression in our spectrum must be  $\nu_2$ , as assigned in the previous PES spectra.<sup>7,8</sup> The complicated structure that Erickson and Ng observed in the PIE curve may be due to autoionizations. Our derived vibrational intervals,  $\Delta G(\nu_2+1/2)$ , are listed in Table II, and are plotted in Fig. 3 as a function of  $\nu_2$ . The vibrational spacings are regular up to  $\nu_2 = 7$ , with a positive anharmonicity. A least-squares fit over this range yields the following spectroscopic constants for  $\nu_2$ :  $\omega_e = 404 \pm 1 \text{ cm}^{-1}$ ,  $\omega_e x_e = 1.5 \pm 0.3 \text{ cm}^{-1}$ . However, the spacings become irregular above  $\nu_2 = 7$ . This suggests that the photoionization transition reaches to the top of the potential barrier (to linearity) in the  $\nu_2$  double-well potential. The potential barrier seriously perturbs the vibrational levels around the barrier maximum. Essentially, a frequency halving will be observed far above the barrier maximum, as is the case in  $H_2S^+(\tilde{A}^2A_1)$ <sup>30</sup> and the first band of  $NF_3^+$ .<sup>31</sup> An irregular vibrational structure will be observed as the transition approaches the barrier maximum. This, in

turn, allows an estimation of the barrier height. If we assume that the  $v_2 = 9$  level lies just above the barrier, we estimate the barrier height to be 0.42 eV ( $3400 \text{ cm}^{-1}$ ) above the zero point energy. For the counterpart state in  $\text{O}_3^+$ , Dyke, Golob, Jonathan, Morris, and Okuda<sup>32</sup> observed a complex vibrational structure at the beginning of the band. They estimated a barrier height to be  $1880 \text{ cm}^{-1}$ . Although their assignment for the onset of the state has been questioned,<sup>20</sup> we believe that the assumption of a potential barrier is reasonable.

b. The Second Band [ $\tilde{\text{A}}^2\text{A}_2$  ( $1a_2^{-1}$ ) and  $\tilde{\text{B}}^2\text{B}_2$  ( $5b_2^{-1}$ ) states]

An expanded spectrum of this band is shown in Fig. 4. It is complex, but the vibrational structure is well resolved. On the high energy side, a  $v_2$  progression is observed, as assigned before.<sup>7,8</sup> Another progression with weak intensity is also resolved in the current spectrum, which was not observed in previous studies.<sup>7-13</sup> The low energy side of the band is much more complicated. Both the previous experiments<sup>7,8</sup> and theoretical calculations<sup>23,27</sup> agreed that this band contained two overlapping states formed by ionizing  $1a_2$  and  $5b_2$  orbitals. For the first state ( $\tilde{\text{A}}^2\text{A}_2$ ), Turner et al.<sup>7</sup> obtained an adiabatic IP of 12.98 eV, while Eland and Danby determined a value of 13.01 eV.<sup>8</sup> At the onset of the band, two small features are resolved in the current spectrum, and the adiabatic IP for the  $\tilde{\text{A}}^2\text{A}_2$  state is measured to be  $12.988 \pm 0.005$  eV. The second state should apparently be the well-developed progression at the high energy side. Turner et al.<sup>7</sup> were not sure where the progression started and did not determine the



adiabatic IP, while Eland and Danby<sup>8</sup> obtained an adiabatic IP of 13.24 eV by assuming that two components of the  $\tilde{B}^2B_2$  state overlapped with the  $\tilde{A}^2A_2$  state. In our high resolution spectrum, we cannot find any peak or shoulder around 13.24 eV. Instead, we assign the overlapping peak at 13.338 eV as the first component of the  $\tilde{B}^2B_2$  state and obtain an adiabatic IP of  $13.338 \pm 0.004$  eV.

The  $\tilde{A}^2A_2$  state will be discussed first. This state was not completely resolved before, and no definite assignment is available. Turner et al.<sup>7</sup> used the combination of  $\nu_2$  and  $2\nu_3$  to assign the spectral features, while Eland and Danby<sup>8</sup> assigned it using  $\nu_1$  and  $\nu_2$ . Cederbaum et al.<sup>22</sup> noticed this "difficult assignment problem" and did a many-body ab initio calculation. They used the vibrational constants reported by Eland and Danby<sup>8</sup> to model a vibrational spectrum. Though this approach produced an irregular vibrational structure, it could not be conclusive, because the experimental resolution was limited (0.035 eV). In fact, it failed to reproduce the small features at the onset of this state that are observed in our spectrum. The spacing between these two weak peaks is  $202(13) \text{ cm}^{-1}$ . The spacing between the second peak and the third sharp peak is  $243(9) \text{ cm}^{-1}$ . Neither of these can be  $\nu_1$  or  $\nu_2$ . It is apparent that there are two  $\nu_2$  progressions starting at the third peak and at the most intense peak (i.e., at the peaks labeled 002 and 004 in Fig. 4). The spacing between these two progressions is  $1467(2) \text{ cm}^{-1}$ . This must correspond to  $2\nu_3$ . Turner et al.<sup>7</sup> did not resolve the first two weak peaks, so they assigned the spacing between the first peak and the most intense peak to be  $2\nu_3$  and obtained a  $2\nu_3$  value of  $1860 \text{ cm}^{-1}$ . The  $\nu_3$  is an asymmetric vibrational mode, and only the even quantum

levels are vibronically allowed.<sup>33</sup> The intensities of such a vibrational mode are normally very low, unless there is a big change of geometry or vibrational frequency in the ionic state.<sup>33</sup> The unusually intense  $\nu_3$  transition in the  $\bar{A}^2A_2$  state here suggests that the  $\bar{A}^2A_2$  state must have been significantly distorted along the  $\nu_3$  coordinate. The first two features of the state should be also taken into account and they should be two early members of the  $\nu_3$  vibration. Therefore, the  $\nu_3$  mode has rather erratic vibrational levels, suggesting that a potential barrier exists in the potential surface along the  $\nu_3$  coordinate. This potential barrier separates two equivalent unsymmetric  $SO_2^+$  ions with the two S-O bonds being unequal ( $C_s$  symmetry). The unusual small spacings of  $\nu_3$  at the beginning of the progression is consistent with being around the barrier maximum. Assuming that only the first level is below the barrier maximum, we estimate the barrier height to be less than  $202\text{ cm}^{-1}$ . The ion is essentially still symmetric above the ground vibrational state, since the potential barrier is so low that with only one quantum of the vibrational energy the ion can overcome the barrier and vibrate back and forth between the two equivalent unsymmetric configurations separated by the potential barrier. A similar situation was observed in the electronic absorption spectrum of  $SO_2$  for the transition  $\bar{C}^1B_2 \leftarrow \bar{A}^1A_1 [b_1(\pi^*) \leftarrow 1a_2(\pi)]$ , where an electron was excited from the  $1a_2$  orbital to the  $b_1$  antibonding orbital.<sup>34</sup> The spectrum was very complicated and the interpretation involved assuming a double well potential along the  $\nu_3$  coordinate. Therefore, the equilibrium geometry of  $SO_2$  in the  $\bar{C}^1B_2$  state was unsymmetric. A subsequent theoretical treatment<sup>35</sup> yielded the barrier height to be  $141\text{ cm}^{-1}$  and the

equilibrium values of the short and long S-O bonds to be 1.491Å and 1.639Å respectively (compared with 1.4321Å for the SO<sub>2</sub> ground state<sup>29</sup>). The calculated energy levels for the  $\nu_3$  mode were  $1\nu_3 = 211 \text{ cm}^{-1}$ ,  $2\nu_3 = 562 \text{ cm}^{-1}$ ,  $3\nu_3 = 891 \text{ cm}^{-1}$ , and  $4\nu_3 = 1249 \text{ cm}^{-1}$ , which are comparable to the  $\nu_3$  energy levels for SO<sub>2</sub><sup>+</sup> ( $\tilde{B}^2A_2$ ) observed in our spectrum, as seen from Table III. As a matter of fact, Jaffe<sup>36</sup> has treated the nonrigid SO<sub>2</sub> molecule in the  $\tilde{C}^1B_2$  state by classical mechanics and reassigned the observed vibrational structure of the  $\tilde{C}^1B_2 \leftarrow \tilde{X}^1A_1$  electronic transition by a set of local modes and normal modes. The  $\tilde{C}^1B_2$  state of SO<sub>2</sub> and the  $\tilde{A}^2A_2$  state of SO<sub>2</sub><sup>+</sup> should have similar properties, since both involve removing an electron from the same orbital ( $1a_2$ ).

The  $\nu_3 = 1$  level is a vibronically forbidden transition without any vibronic interaction.<sup>33</sup> Such a transition was also observed in other molecules.<sup>37</sup> The  $\nu_1$  mode must also be taken into account in order to make a thorough assignment for this state. The complete assignment is shown in Fig. 4, and the IP's and vibrational intervals are listed in Table III. The  $\nu_3 = 3$  transition may also contribute to the broad feature at 13.11 eV.

The assignment for the  $\tilde{B}^2B_2$  state is straightforward. Both Turner et al.<sup>7</sup> and Eland and Danby<sup>8</sup> assigned this state with a pure  $\nu_2$  vibration. The calculation of Cederbaum et al. with a pure  $\nu_2$  mode reproduced this state well.<sup>27</sup> Moreover, their calculated band maximum agrees with our assignment. The derived  $\Delta G(\nu_2+1/2)$  values are listed in Table IV. A least-squares fitting of  $\Delta G(\nu_2+1/2)$  vs  $\nu_2$  yields the following spectroscopic constants:  $\omega_e = 489 \pm 5 \text{ cm}^{-1}$ ,  $\omega_e x_e = 2 \pm 1 \text{ cm}^{-1}$ . However, it can be seen from Table IV or Fig. 5 that the vibrational

intervals do not decrease monotonically as a function of  $v_2$  within the experimental uncertainty.

A new progression with relatively low intensity is resolved for the  $\tilde{B}^2B_2$  state in Fig. 4. This is another  $v_2$  progression, which should be a combination of  $v_2$  with either  $v_1$  or  $v_3$ . The difference between this progression and the main progression is  $1223\text{ cm}^{-1}$ , which cannot be  $v_1$  ( $1151.3\text{ cm}^{-1}$  for  $\text{SO}_2^{29}$ ). We assign it to be  $2v_3$  since  $1v_3$  is normally forbidden.<sup>33</sup> The fact that the  $v_3$  mode is active suggests that the  $\tilde{B}^2B_2$  state is also somehow distorted along the  $v_3$  coordinate. Since the  $\tilde{B}^2B_2$  and  $\tilde{A}^2A_2$  states are formed by ionizing  $1a_2$  and  $5b_2$  orbitals, both of which are originated from the S d-orbital bonding, there is no surprise that the two states have some similar characteristics. They are both distorted along both  $v_2$  and  $v_3$  coordinates, and both have very different geometries from the ground state. The  $\tilde{A}^2A_2$  state is distorted more along the  $v_3$  coordinate, and the  $\tilde{B}^2B_2$  state is distorted more along the  $v_2$  coordinate. Therefore, from the Franck-Condon principle, the major vibrational progression should be  $v_3$  for the  $\tilde{A}^2A_2$  state, and  $v_2$  for the  $\tilde{B}^2B_2$  state. However, it is not clear from our spectrum whether the  $\tilde{B}^2B_2$  state also has an asymmetric equilibrium geometry like the  $\tilde{A}^2A_2$  state. From the fact that the  $v_2$  mode in the  $\tilde{B}^2B_2$  state has an abnormal spacing dependence with  $v_2$ , it is clear that the  $v_3$  mode couples with the  $v_2$  mode in the  $\tilde{B}^2B_2$  state so that the  $v_2$  mode differs from a normal anharmonic oscillator, as shown in Fig. 5.

c. The Third Band [ $\tilde{C}^2B_2$  ( $4b_2^{-1}$ ),  $\tilde{D}^2A_1$  ( $7a_1^{-1}$ ), and  $\tilde{E}^2B_1$  ( $2b_1^{-1}$ )]

This band is shown separately in Fig. 6. The spectrum is diffuse at the high IP side, which makes the assignment more difficult. In the early PES studies of  $\text{SO}_2^+$ , some inconsistency arose about the number of states in the band. Turner et al.<sup>7</sup> and Eland and Danby<sup>8</sup> assigned only two states in their early studies. It was Lloyd and Roberts<sup>9</sup> who first assigned the third state from a higher resolution study. Their assignment was  $\tilde{C}^2B_2$ ,  $\tilde{D}^2A_1$ ,  $\tilde{E}^2B_1$ , obtained by comparing their experimental evidence with Hillier and Saunders's ab initio SCFMO calculation.<sup>23</sup>

For the  $\tilde{C}^2B_2$  state, both  $\nu_1$  and  $\nu_2$  modes are excited. As pointed out earlier, we observed the true adiabatic transition for this state. This allows us to observe  $\nu_1$  up to  $\nu_1 = 8$ , which we believe is the complete Franck-Condon region for the  $\tilde{C}^2B_2$  state. The derived vibrational intervals,  $\Delta G(\nu_1+1/2)$ , are shown in Table V. A least-squares fit of  $\Delta G(\nu_1+1/2)$  vs  $\nu_1$  yields the following spectroscopic constants for  $\nu_1$ :  $\omega_e = 816 \pm 3 \text{ cm}^{-1}$ ,  $\omega_e x_e = 3 \pm 0.5 \text{ cm}^{-1}$ . The average  $\nu_2$  value is  $365 \pm 3 \text{ cm}^{-1}$ . The  $\tilde{D}^2A_1$  and  $\tilde{E}^2B_1$  state are assigned with the  $\nu_1$  mode only. It is difficult to make a thorough assignment, and to find the spectroscopic constants for these two states by the routine least-squares fitting method, since the spectrum becomes rather diffuse toward the high energy side. The vibrational spacings which can be determined are listed in Table VI.

The broadened spectrum indicates fast dynamic processes occurring in this band. The dissociation limits of  $\text{SO}_2^+$  to form  $\text{SO}^+ + \text{O}$  and  $\text{S}^+ + \text{O}_2$  in their ground states are 15.95 eV and 16.23 eV respectively.<sup>20</sup> These are the only two dissociation channels which can occur in this band. Three

accounts have been given of the dissociation mechanisms for the ion.<sup>14-16</sup> From their threshold photoelectron-photoion coincidence experiment, Weiss, Hsieh, and Meisels<sup>15</sup> observed that  $S^+$  was only formed in a very narrow energy range between 16.334-16.674 eV and that  $SO_2^+$  became fully predissociated above about 16.67 eV in this band. They explained the formation of  $SO^+$  and  $S^+$  by using a vibrational predissociation model in the  $\tilde{C}^2B_2$  state. Dujardin and Leach<sup>16</sup> made a photoion-fluorescence photon coincidence measurement and concluded that  $S^+$  could not be formed in the  $\tilde{C}^2B_2$  state, but must come from a higher state. They observed fluorescence in coincidence with  $SO_2^+$  in the third band with a small quantum yield.

It has been shown that a high resolution photoelectron spectrum can be useful in understanding the ultrafast dynamics of a molecular ion, through the correlation functions obtained by Fourier transformations of the individual electronic bands in the photoelectron spectrum.<sup>3b,37,38</sup> In the case of the third band of  $SO_2^+$ , the strong overlapping of the three electronic states precludes obtaining the correlation functions. However, the dynamical information that a photoelectron spectrum carries does not depend on the correlation functions. In high resolution PES, the instrumental function limits the time scale on which the ultrafast dynamics can be measured. With an instrumental resolution of 13 meV, we obtain an upper limit of 51 fs for this time scale from the time-energy uncertainty principle. In other words, any state with a lifetime shorter than 51 fs will broaden the spectrum. Therefore, the spectral diffuseness signals the presence of ultrafast processes, from which the dynamics can be inferred.

In the third band of  $\text{SO}_2^+$ , the spectrum becomes considerably broadened above about 16.7 eV, which means the ultrafast dissociation starts around 16.7 eV. The spectrum below 16.7 eV essentially represents the instrumental resolution, indicating that the states below 16.7 eV have lifetimes longer than 51 fs, that is, the  $\tilde{\text{C}}$  state is relatively stable as it covers this whole range. This is consistent with the observation of fluorescence from this region of the spectrum, which gave a lifetime of less than 10 ns.<sup>16</sup> This also agrees with Weiss et al.'s experiment,<sup>15</sup> which shows that  $\text{SO}_2^+$  is completely predissociated above 16.67 eV.<sup>15</sup> However, it has been observed that the ion does dissociate from the  $\tilde{\text{C}}^2\text{B}_2$  state, and various interpretations<sup>14-16</sup> have been given to the dissociation mechanisms. The ion can not directly dissociate through this state, since that would require the  $\tilde{\text{C}}^2\text{B}_2$  state to have a very shallow potential well.<sup>16</sup> Therefore, the dissociations from the  $\tilde{\text{C}}$  state have to proceed through the lower lying states, by electronic predissociations. Because  $\text{SO}_2^+$  is a small molecule and there is a big  $\tilde{\text{C}}-\tilde{\text{B}}$  state energy gap, these predissociations are unfavored. It is these unfavored processes that actually lengthen the lifetime of the state so that the fluorescence is competitive with the predissociations.

The combination of the  $\text{SO}^+(\tilde{\text{X}}^2\Pi) + \text{O}(^3\text{P}_g)$  product states can lead to twelve states in the  $\text{C}_s$  molecular symmetry. These twelve states [ $3(^2,^4\text{A}')$  and  $3(^2,^4\text{A}'')$ ] can correlate, in the  $\text{C}_{2v}$  point group, with all four possible species  $\text{A}_1$ ,  $\text{A}_2$ ,  $\text{B}_1$ , and  $\text{B}_2$ . We propose that the formation of  $\text{SO}^+ + \text{O}$  occurs through a predissociation by the  $\tilde{\text{A}}^2\text{A}_2$  state, which possesses an asymmetric ground state geometry favorable to the asymmetric dissociation. However, in the formation of  $\text{S}^+ + \text{O}_2$ , the

whole molecular symmetry ( $C_{2v}$ ) is retained, and combination of the products in their ground states yields states of  $6, 4, 2B_2$  symmetry. Therefore, the dissociation to  $S^+ + O_2$  must be through a predissociation of the  $\tilde{C} \ 2B_2$  state by the  $\tilde{B} \ 2B_2$  state, which is observed to be strongly deformed along the  $\nu_2$  vibration favorable to form  $S^+ + O_2$ . As Weiss et al. originally<sup>15</sup> proposed,  $S^+$  is produced entirely from the  $\tilde{C} \ 2B_2$  state. From our spectrum, this would explain why  $S^+$  was only observed in a narrow energy range, since it is simply out of the Franck-Condon region of the  $\tilde{C}$  state above 16.67 eV.

The  $\tilde{D}$  and  $\tilde{E}$  states are responsible for the fast dissociations above 16.7 eV, as evidenced by the spectral diffuseness. In the lack of any theoretical calculation, the only dissociation pathway we can suggest would be predissociations through the  $\tilde{C} \ 2B_2$  state, since the spectral feature precludes any direct dissociation model.

#### d. The CI Bands

Two weak bands which occur at about 14.6 and 17.5 eV were interpreted by Kimura et al. as two CI bands.<sup>12</sup> Vibrational structure is resolved in the current spectrum, as seen from Fig. 1 and Fig. 6. It turns out that the band at 14.6 eV is the HeI  $\beta$  line spectrum of the third band. The band at 17.5 eV must be a true CI band, because the  $\tilde{F} \ 2A_1$  state is at 20.06 eV<sup>9,11</sup> and the  $\beta$  line spectrum would occur at a higher energy. CI bands are well known in the photoionization of the inner shell electrons for the first and second row molecules,<sup>39</sup> and CI bands in the valence region have been observed in other third row



molecules.<sup>40</sup> The band we observed consists of two  $\nu_1$  vibrational progressions which may be two components of a spin-orbit split state. The energies and spacings are listed in Table VII. Autoionization was proposed for this band,<sup>11</sup> but the sharpness of the vibrational structure excludes this possibility.

V SUMMARY

Our high resolution PES study of  $\text{SO}_2$  using supersonic molecular beams allows accurate adiabatic IP's for the first six states of  $\text{SO}_2^+$  to be determined. The vibrational structure is explicitly resolved in all observed states. The  $\tilde{X}^2A_1$  state is assigned to  $\nu_2$  vibrations exclusively. A potential barrier is proposed to interpret the irregular vibrational structure on the high energy side. The barrier height for the  $\tilde{X}^2A_1$  state is estimated to be 0.42 eV ( $3400 \text{ cm}^{-1}$ ). The complex second band contains two states. The abnormal vibrational structure in the  $\tilde{A}^2A_2$  state is explained by the distortion motion along the  $\nu_3$  coordinate upon photoionization, which makes the  $\nu_3$  mode the principal vibration in the state. A potential barrier exists along the  $\nu_3$  coordinate, so that the ion has an asymmetric equilibrium geometry. The barrier height for the  $\tilde{A}$  state is estimated to be less than  $220 \text{ cm}^{-1}$ . A new progression is resolved in the  $\tilde{B}^2B_2$  state, which is assigned to be the combination of  $\nu_2$  with  $2\nu_3$ . The true adiabatic IP for the  $\tilde{C}^2B_2$  state is determined in the first time to be  $15.902 \pm 0.003 \text{ eV}$ . The decay of this state is discussed and predissociations through the lower lying states are suggested. The spectrum above 16.7 eV is much broadened, suggesting that rapid dissociations occur from the  $\tilde{D}^2A_1$  and  $\tilde{E}^2B_1$  states. Predissociations by the  $\tilde{C}^2B_2$  state are proposed.

We believe that more sophisticated calculations are desirable to compare with the experimental observations, in order to gain a quantitative understanding of the geometry, spectroscopy, and dynamics of the  $\text{SO}_2^+$  ion.

REFERENCES

1. See for example: a. Molecular Ions: Geometric and Electronic Structures, edited by J. Berkowitz and K.O. Groenveld (Plenum, N.Y., 1983). b. Molecular Ion Studies. A special issue of J. Chim. Phys. 77, 585-777 (1980), edited by S. Leach. c. Molecular Ions: Spectroscopy, Structure, and Chemistry, edited by T.A. Miller and V.E. Bondybey (North-Holland, Amsterdam, 1983)
2. J.E. Pollard, D.J. Trevor, J.E. Reutt, Y.T. Lee, and D.A. Shirley, J. Chem. Phys. 77, 34 (1982)
3. a. J.E. Pollard, D.J. Trevor, J.E. Reutt, Y.T. Lee, and D.A. Shirley, J. Chem. Phys. 81, 5302 (1984)  
b. J.E. Reutt, L.S. Wang, Y.T. Lee, and D.A. Shirley, J. Chem. Phys. 85, 6928 (1986).
4. a. H.D. Smyth, and D.W. Mueller, Phys. Rev. 43, 121 (1933).  
b. R.M. Reese, V.H. Dibeler, and J.L. Franklin, J. Chem. Phys. 29, 880 (1958).  
c. R. Hagemann, C. R. Acad. Sci. 255, 1102 (1962).  
d. R. Botter, R. Hagemann, G. Nief, and E. Roth, Advances in mass Spectrometry (The Institute of Petroleum, London, 1966), Vol. 3, P 951.
5. C.E. Brion and D.S.C. Yee, J. Electron Spectros. Relat. Phenom. 12, 77 (1977)
6. a. W.C. Price and D.M. Simpson, Proc. R. Soc. (London) A165, 272 (1938).  
b. D. Golomb, K. Watanabe, and F.F. Marmo, J. Chem. Phys. 36, 958,

(1962).

7. D.W. Turner, C. Baker, A.D. Baker, and C.R. Brundle, Molecular Photoelectron Spectroscopy (Wiley-Interscience, London, 1970).
8. J.H.D. Eland and C.J. Danby, *Int. J. Mass Spectrom. Ion Phys.* 1, 111 (1968).
9. D.R. Lloyd and P.J. Roberts, *Mol. Phys.* 26, 225 (1973).
10. H. Bock, B. Solouki, P. Rosmus, R. Steudel, and W. Schultheis, *Angew. Chem.* 85, 987 (1973).
11. A.W. Potts, *J. Electron Spectros. Relat. Phenom.* 11, 157 (1977).
12. K. Kimura, S. Katsumata, Y. Achiba, T. Yamazaki, and S. Iwata, Handbook of HeI Photoelectron Spectra of Fundamental Organic Molecules (Japan Scientific Societies Press, 1981).
13. D.M.P. Holland, A.C. Parr, and J.L. Dehmer, *J. Electron Spectros. Relat. Phenom.* 32, 237 (1983).
14. B. Brehm, J.H.D. Eland, R. Frey, and A. Kustler, *Int. J. Mass Spectrom. Ion Phys.* 12, 197 (1973).
15. M.J. Weiss, T.C. Hsieh, and G.G. Meisels, *J. Chem. Phys.* 71, 567 (1979).
16. G. Dujardin and S. Leach, *J. Chem. Phys.* 76, 2521 (1981).
17. E.C.Y. Inn, *Phys. Rev.* 91, 1194 (1953).
18. K. Watanabe, *J. Chem. Phys.* 26, 542 (1957).
19. V.H. Dibeler and S.K. Liston, *J. Chem. Phys.* 49, 482 (1968).
20. J. Erickson and C.Y. Ng, *J. Chem. Phys.* 75, 1650 (1981).
21. C.Y.R. Wu and C.Y. Ng, *J. Chem. Phys.* 76, 4406 (1982).
22. G. Herzberg, Infrared and Raman Spectra of Polyatomic Molecules (Van Nostrand Reinhold Company Inc., 1945), P 285.

23. I.H. Hillier and V.R. Saunders, *Mol. Phys.* 22, 193 (1971).
24. S. Rothenberg and H.F. Schaefer III, *J. Chem. Phys.* 53, 3014 (1970).
25. J.G. Norman, Jr, *Mol. Phys.* 31, 1191 (1976).
26. L. Noodleman and K.A.R. Mitchell, *Inorg. Chem.* 17, 2709 (1978).
27. L.S. Cederbaum, W. Domcke, W.V. Niessen and W.P. Kraemer, *Mol. Phys.* 34, 381 (1977).
28. J.E. Pollard, D.J. Trevor, Y.T. Lee, and D.A. Shirley, *Rev. Sci. Instrum.* 52, 1837 (1981).
29. G. Herzberg, Electronic Spectra and Electronic Structures of Polyatomic Molecules (Litton Educational Publishing, Inc., 1966) P 605.
30. L. Karlsson, L. Mattsson, R. Jadrny, T. Bergmark, and K. Siegbahn, *Phys. Scr.* 13, 229 (1976).
31. J. Berkowitz and J.P. Greene, *J. Chem. Phys.* 81, 3383 (1984).
32. J.M. Dyke, L. Golob, N. Jonathan, A. Morris, and M. Okuda, *J. Chem. Soc. Faraday Trans. 2*, 70, 1828 (1974).
33. J.R. Rabalais, Principle of Ultraviolet Photoelectron Spectroscopy (John Wiley & Sons, Inc., 1977), P 70.
34. a. V.T. Jones and J.B. Coon, *J. Mol. Spectros.* 47, 45 (1973).  
b. J.C.D. Brand, P H. Chiu, and A.R. Hoy, *J. Mol. Spectros.* 69, 43 (1976).
35. A.R. Hoy and J.C.D. Brand, *Mol. Phys.* 36, 1409 (1978).
36. C. Jaffe, *J. Chem. Phys.* 81, 616 (1984).
37. a. J.E. Pollard, D.J. Trevor, J.E. Reutt, Y.T. Lee. and D.A. Shirley, *J. Chem. Phys.* 81, 5302 (1984).

- b. R. McDiarmid, J. Phys. Chem. 84, 64 (1980).
38. A.J. Lorquet, J.C. Lorquet, J. Delwiche, and M.T. Hubin-Franskin, J. Chem. Phys. 76, 4692 (1982).
39. A.W. Potts and T.A. Williams, J. Electron Spectros. Relat. Phenom. 3, 3 (1974).
40. I. Reineck, B. Wannberg, H. Veenhuizen, C. Nohre, R. Maripuu, K.E. Nozell, L. Mattsson, L. Karlsson, and K. Siegbahn, J. Electron Spectros. Relat. Phenom. 34, 235 (1984).

#### ACKNOWLEDGEMENTS

This work was supported by the Director, Office of Energy Research, Office of Basic Energy Sciences, Chemical Science Division of the U.S. Department of Energy under Contract No. DE-AC03-76SF00098.

Table I. Adiabatic ionization potentials of the first seven electronic states of  $\text{SO}_2^+$  (eV).

	$\tilde{X}^2A_1$	$\tilde{A}^2A_2$	$\tilde{B}^2B_2$	$\tilde{C}^2B_2$	$\tilde{D}^2A_1$	$\tilde{E}^2B_1$	$\tilde{F}^2A_1$
a	12.349(3)	12.988(5)	13.338(4)	15.902(3)	16.339(3)	16.507(3)	
b	12.29	12.98		15.97	16.33		
c	12.30	13.01	13.24	15.986	16.326	(16.7)	
d				15.992	16.324	16.498	20.06
e	12.348(2)						

a. This work.

b. Turner et al. From reference 7.

c. Eland and Danby. From reference 8.

d. Lloyd and Roberts. From reference 9.

e. Erickson and Ng. From reference 20.

Table II. Ionization potentials (eV), vibrational frequencies ( $\text{cm}^{-1}$ ) and the assignment for the  $\tilde{X}^2A_1$  state of  $\text{SO}_2^+$ .

IP	assignment <sup>a</sup>	$\Delta G(v_2+1/2)$
12.2856(7) <sup>b</sup>	<sup>1</sup> 2 <sub>0</sub> hot band	
12.3494(2)	0 0 0	515(3)
12.3995(2)	0 1 0	404.2(0.5) <sup>c</sup>
12.4493(2)	0 2 0	401.8(0.5) <sup>c</sup>
12.4985(2)	0 3 0	396.9(0.5) <sup>c</sup>
12.5474(2)	0 4 0	394.5(0.5) <sup>c</sup>
12.5960(2)	0 5 0	392.1(0.5) <sup>c</sup>
12.6443(2)	0 6 0	389.7(0.5) <sup>c</sup>
12.6923(2)	0 7 0	387.3(1.0) <sup>c</sup>
12.7382(4)	0 8 0	370.3(2)
12.7697(9)	0 9 0	254.1(8)
12.7878(10)	0 10 0	146.0(11)

- a. The assignment is labelled with the quantum numbers of  $v_1$ ,  $v_2$ ,  $v_3$ .
- b. The uncertainties of the absolute IP'S are  $\pm 0.003$  eV. The smaller uncertainties quoted refer to the relative positions of the transitions, which are used to calculate the uncertainties for the vibrational splittings.
- c. Values used in the least-squares fitting.



Table III. Ionization potentials (eV), vibrational frequencies ( $\text{cm}^{-1}$ ) and the assignment for the  $\tilde{A}^2A_2$  state of  $\text{SO}_2^+$ .

IP	assignment <sup>a</sup>	$\nu_1$	$\Delta G(\nu_2+1/2)$	$\nu_3$
12.9884(21) <sup>b</sup>	0 0 0			
13.0134(21)	0 0 1			202(13)
13.0435(6)	0 0 2			243(9)
13.0873(10)	0 1 2		353(7)	
13.1100(82)	1 0 0	981(60)		
13.1255(98)	1 0 1	904(71)		
13.1436(33)	0 2 2		452(15)	
13.1730(19)	1 0 2	1045(10)		
13.1894(80)	0 3 2		370(60)	
13.2253(6)	0 0 4			1466.8(1.4) <sup>c</sup>
13.2749(6)	0 1 4		400.2(1.6)	
13.3236(23)	0 2 4		393(18)	
13.3569(8)	1 0 4	1062(5)		
13.3730(13)	0 3 4		399(9)	
13.4120(31)	0 4 4		315(12)	

a. The assignment is labelled with the quantum numbers of  $\nu_1$ ,  $\nu_2$ ,  $\nu_3$ .

b. See (b) in Table II.

c.  $2\nu_3$  value.

Table IV. Ionization potentials (eV), vibrational frequencies ( $\text{cm}^{-1}$ ) and the assignment for the  $\tilde{B}^2B_2$  state of  $\text{SO}_2^+$ .

IP	assignment <sup>a</sup>	$\Delta G(v_2+1/2)$	$2v_3$
13.3384(12) <sup>b</sup>	0 0 0		
13.3960(7)	0 1 0	465(9)	
13.4578(6)	0 2 0	499(4)	
13.4900(50)	0 0 2		1223(13)
13.5169(7)	0 3 0	477(1)	
13.5503(10)	0 1 2		1245(8)
13.5775(6)	0 4 0	489(1)	
13.6131(31)	0 2 2		1253(24)
13.6360(6)	0 5 0	472(2)	
13.6657(7)	0 3 2		1201(3)
13.6952(6)	0 6 0	478(2)	
13.7279(8)	0 4 2		1213(5)
13.7538(6)	0 7 0	473(2)	
13.7856(7)	0 5 2		1207(5)
13.8113(6)	0 8 0	464(2)	
13.8459(9)	0 6 2		1216(6)
13.8700(7)	0 9 0	474(2)	
13.9059(9)	0 7 2		1227(7)
13.9277(8)	0 10 0	466(2)	
13.9611(14)	0 8 2		1209(10)
13.9826(15)	0 11 0	443(12)	

14.0232(34)	0 9 2		1236(15)
14.0309(20)	0 12 0	390(20) <sup>c</sup>	
14.0800(140)	0 10 2		1229(43)
14.0891(150)	0 13 0	470(45) <sup>c</sup>	

---

- a. The assignment is labelled with the quantum numbers of  $\nu_1, \nu_2, \nu_3$ .
- b. See (b) in Table II.
- c. Values not used in the least-squares fitting.

Table V. Ionization potentials (eV), vibrational frequencies ( $\text{cm}^{-1}$ ), and the assignment for the  $\tilde{C}^2B_2$  state of  $\text{SO}_2^+$ .

IP	assignment <sup>a</sup>	$\Delta G(v_1+1/2)$	$\nu_2$
15.9020(9) <sup>b</sup>	0 0 0		
15.9480(13)	0 1 0		371(10)
16.0012(8)	1 0 0	800(4)	
16.0468(8)	1 1 0		368(4)
16.1011(8)	2 0 0	806(2)	
16.1460(8)	2 1 0		362(2)
16.1999(8)	3 0 0	797(2)	
16.2441(8)	3 1 0		357(2)
16.2983(7)	4 0 0	794(1)	
16.3956(7)	5 0 0	785(1)	
16.4922(10)	6 0 0	779(5)	
16.5860(80)	7 0 0	757(20) <sup>c</sup>	
16.6240(50)	7 1 0		310(46)

a. The assignment is labelled with the quantum numbers of  $\nu_1$ ,  $\nu_2$ ,  $\nu_3$ .

b. See (b) in Table II.

c. Value not used in the least-squares fitting.

Table VI. Ionization potentials (eV), vibrational frequencies ( $\text{cm}^{-1}$ ) and the assignment for the  $\tilde{D}^2A_1$  and  $\tilde{E}^2B_1$  states of  $\text{SO}_2^+$ .

IP	assignment <sup>a</sup>	$\Delta G(v_1+1/2)^b$	$\Delta G(v_1+1/2)^c$
<sup>b</sup> 16.3393(7) <sup>d</sup>	0 0 0		
<sup>b</sup> 16.4523(7)	1 0 0	912(0.7)	
<sup>c</sup> 16.5074(8)	0 0 0		
<sup>b</sup> 16.5601(8)	2 0 0	869(1)	
<sup>c</sup> 16.5949(9)	1 0 0		706(4)
<sup>b</sup> 16.6580(60)	3 0 0	790(25)	
<sup>c</sup> 16.6858(20)	2 0 0		
<sup>b</sup> 16.7415(10)	4 0 0		
<sup>c</sup> 16.7813(30)	3 0 0		

a. The assignment is labelled with the quantum numbers of  $v_1, v_2, v_3$ .

b. For the  $\tilde{D}^2A_1$  state.

c. For the  $\tilde{E}^2B_1$  state.

d. See (b) in Table II.

Table VII. Ionization potentials (eV), vibrational frequencies ( $\text{cm}^{-1}$ ) and the assignment for the CI band.

IP	assignment <sup>a</sup>	$\Delta G(\nu_1+1/2)^b$	$\Delta G(\nu_1+1/2)^c$
<sup>b</sup> 17.2575(9) <sup>d</sup>	0 0 0		
<sup>b</sup> 17.3783(9)	1 0 0	975(10)	
<sup>c</sup> 17.4261(20)	0 0 0		
<sup>b</sup> 17.5006(9)	2 0 0	987(5)	
<sup>c</sup> 17.5478(10)	1 0 0		982(18)
<sup>b</sup> 17.6184(8)	3 0 0	950(5)	
<sup>c</sup> 17.6648(10)	2 0 0		944(10)
<sup>b</sup> 17.7342(8)	4 0 0	934(14)	
<sup>c</sup> 17.7725(10)	3 0 0		869(10)
<sup>b</sup> 17.8429(10)	5 0 0	877(7)	
<sup>c</sup> 17.8684(20)	4 0 0		774(13)
<sup>b</sup> 17.9472(23)	6 0 0	842(19)	
<sup>c</sup> 17.9718(13)	5 0 0		834(14)
<sup>c</sup> 18.076(10)	6 0 0		840(10)
<sup>c</sup> 18.176(20)	7 0 0		808(17)

a. The assignment is labelled with the quantum numbers of  $\nu_1$ ,  $\nu_2$ ,  $\nu_3$ .

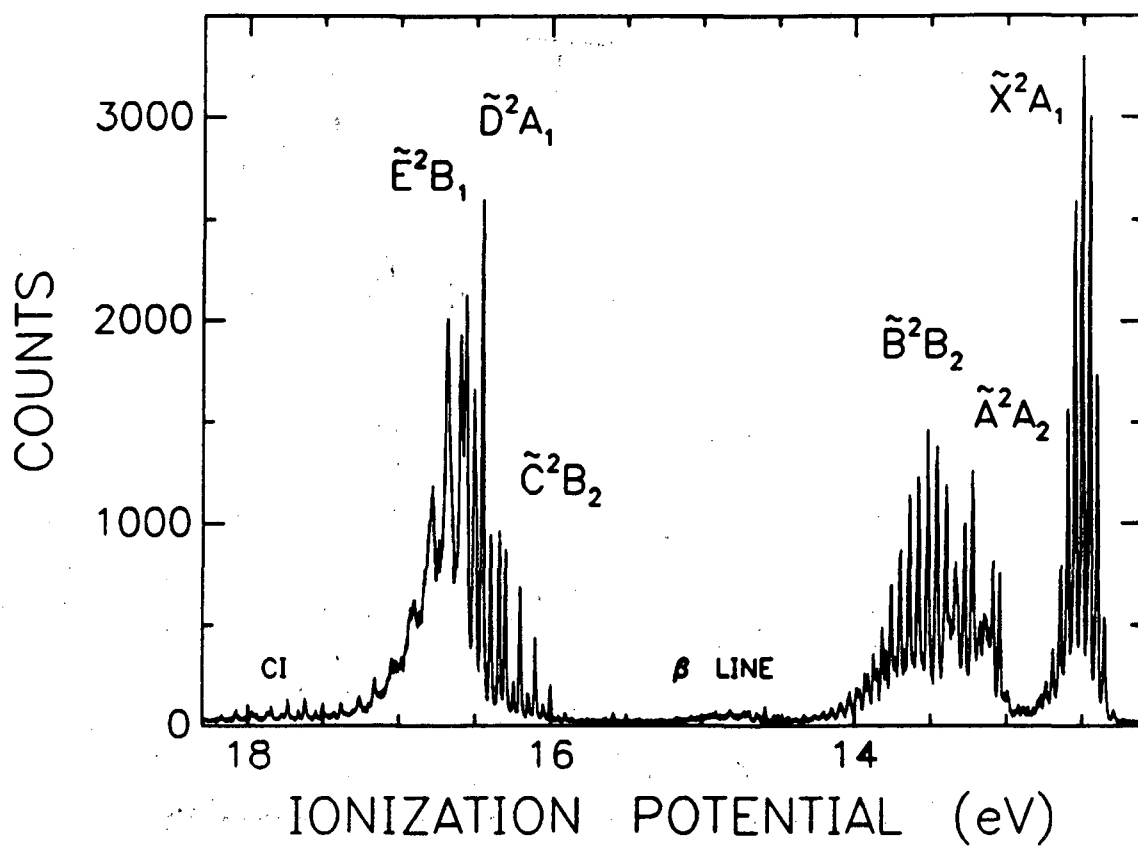
b. For progression 1.

c. For progression 2.

d. See (b) in Table II.

## FIGURE CAPTIONS

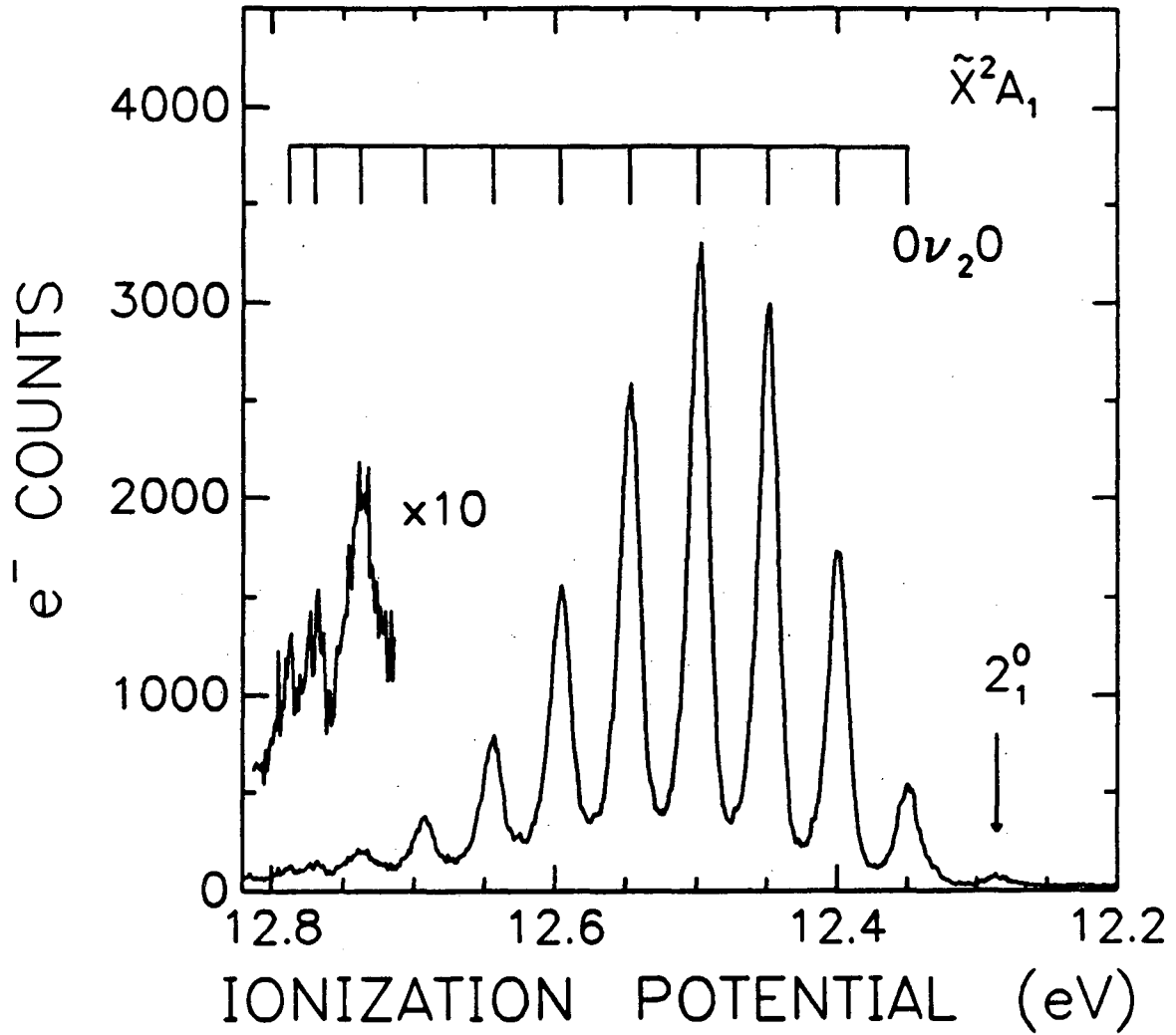
- Figure 1. The complete HeI (584Å) photoelectron spectrum of  $\text{SO}_2^+$  measured with a resolution of 13 meV and a supersonic molecular beam of  $\text{SO}_2$ .
- Figure 2. The first band ( $\tilde{X}^2A_1$  ground state) of the  $\text{SO}_2^+$  HeI photoelectron spectrum and the assignment.
- Figure 3. The vibrational spacing,  $\Delta G(v_2+1/2)$ , of  $v_2$  in the  $\tilde{X}^2A_1$  state as a function of the vibrational quantum number,  $v_2$ .
- Figure 4. The second band ( $\tilde{A}^2A_2$  and  $\tilde{B}^2B_2$  states) of the  $\text{SO}_2^+$  HeI photoelectron spectrum and the assignment.
- Figure 5. The vibrational spacing,  $\Delta G(v_2+1/2)$ , of  $v_2$  in the  $\tilde{B}^2B_2$  state as a function of the vibrational quantum number,  $v_2$ .
- Figure 6. The CI band and the third band ( $\tilde{C}^2B_2$ ,  $\tilde{D}^2A_1$ , and  $\tilde{E}^2B_1$  states) of the  $\text{SO}_2^+$  HeI photoelectron spectrum and the assignment.



XBL 8611-4768

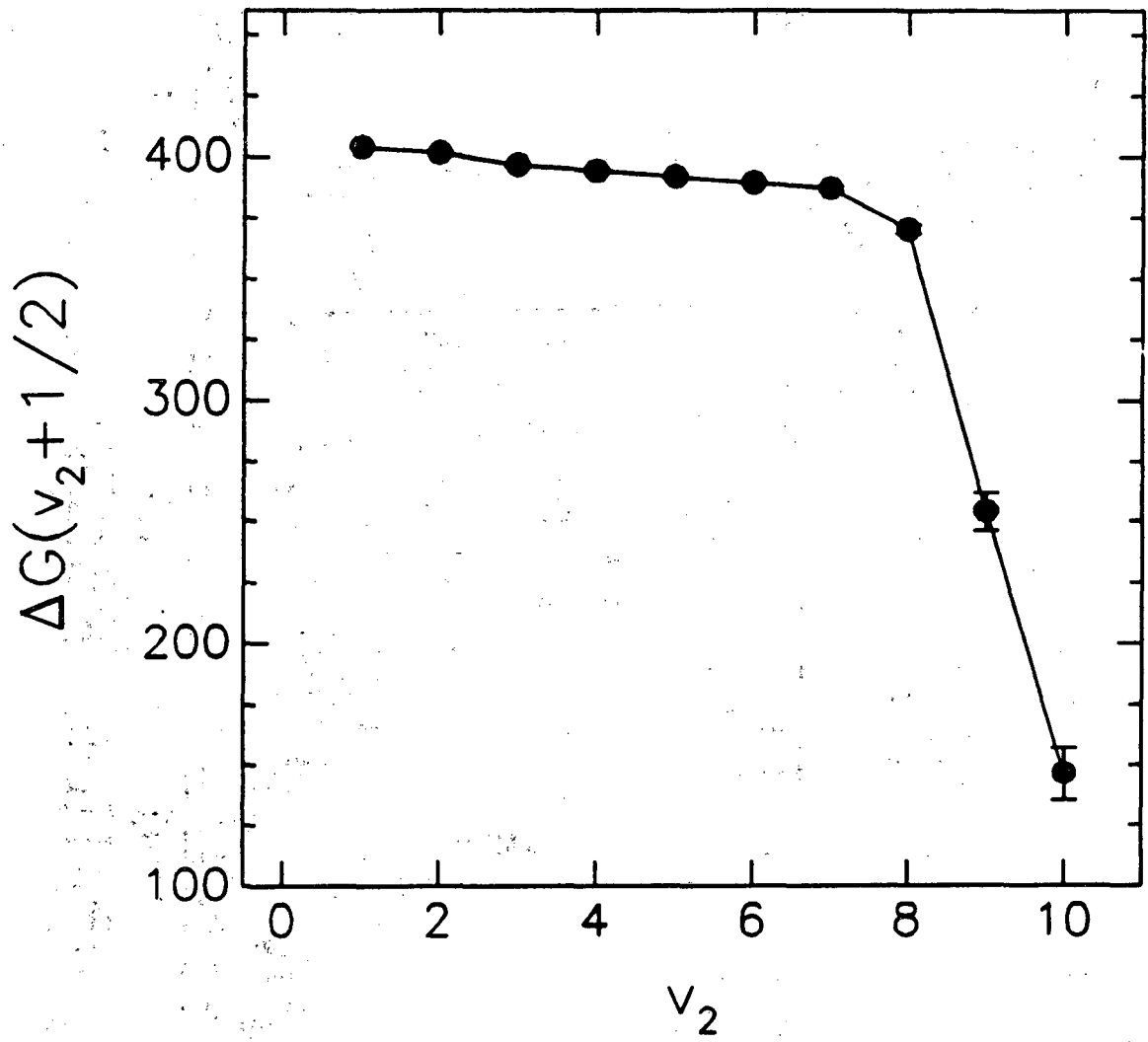
Fig. 1





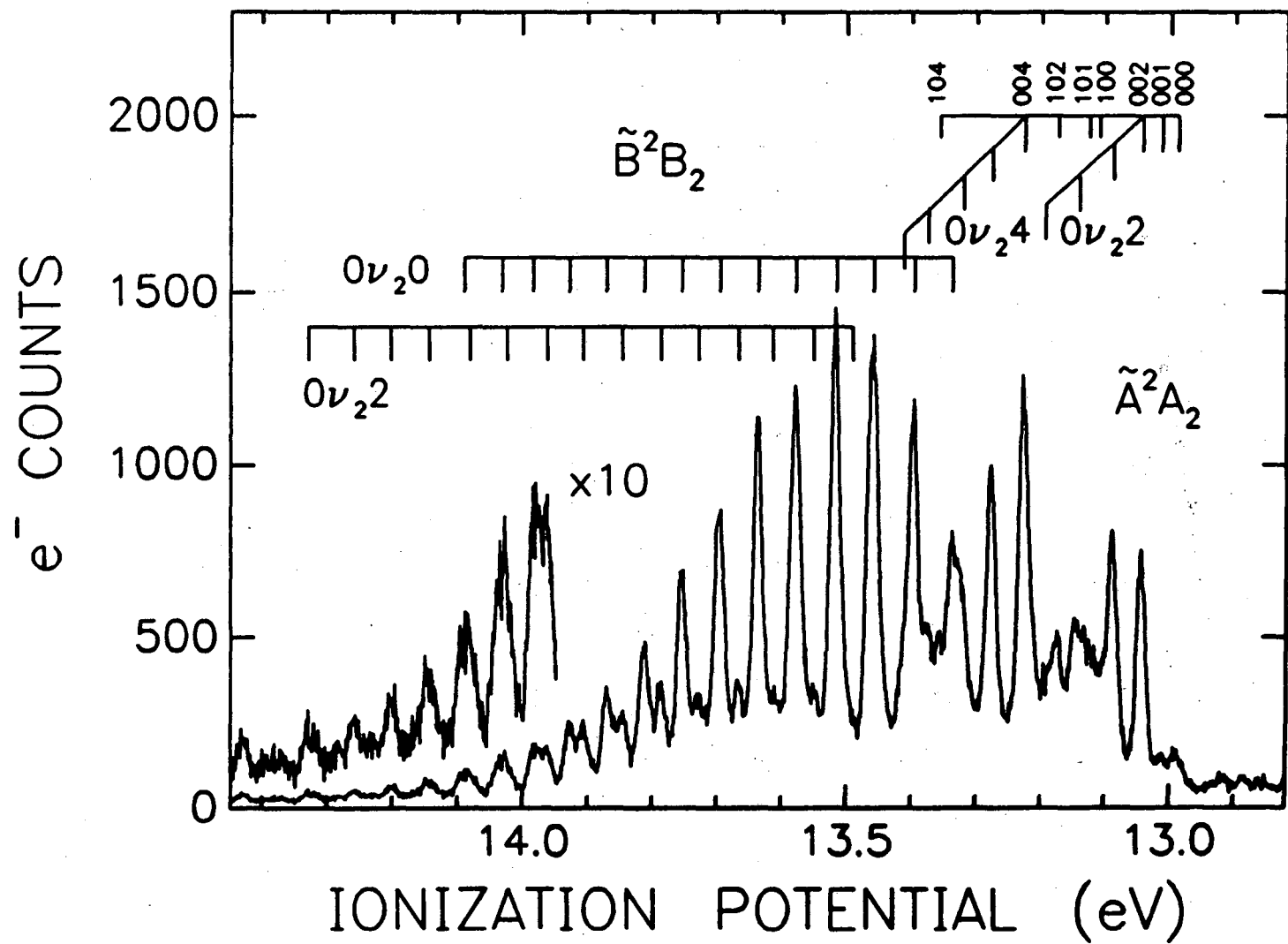
XBL 8611-4769

Fig. 2



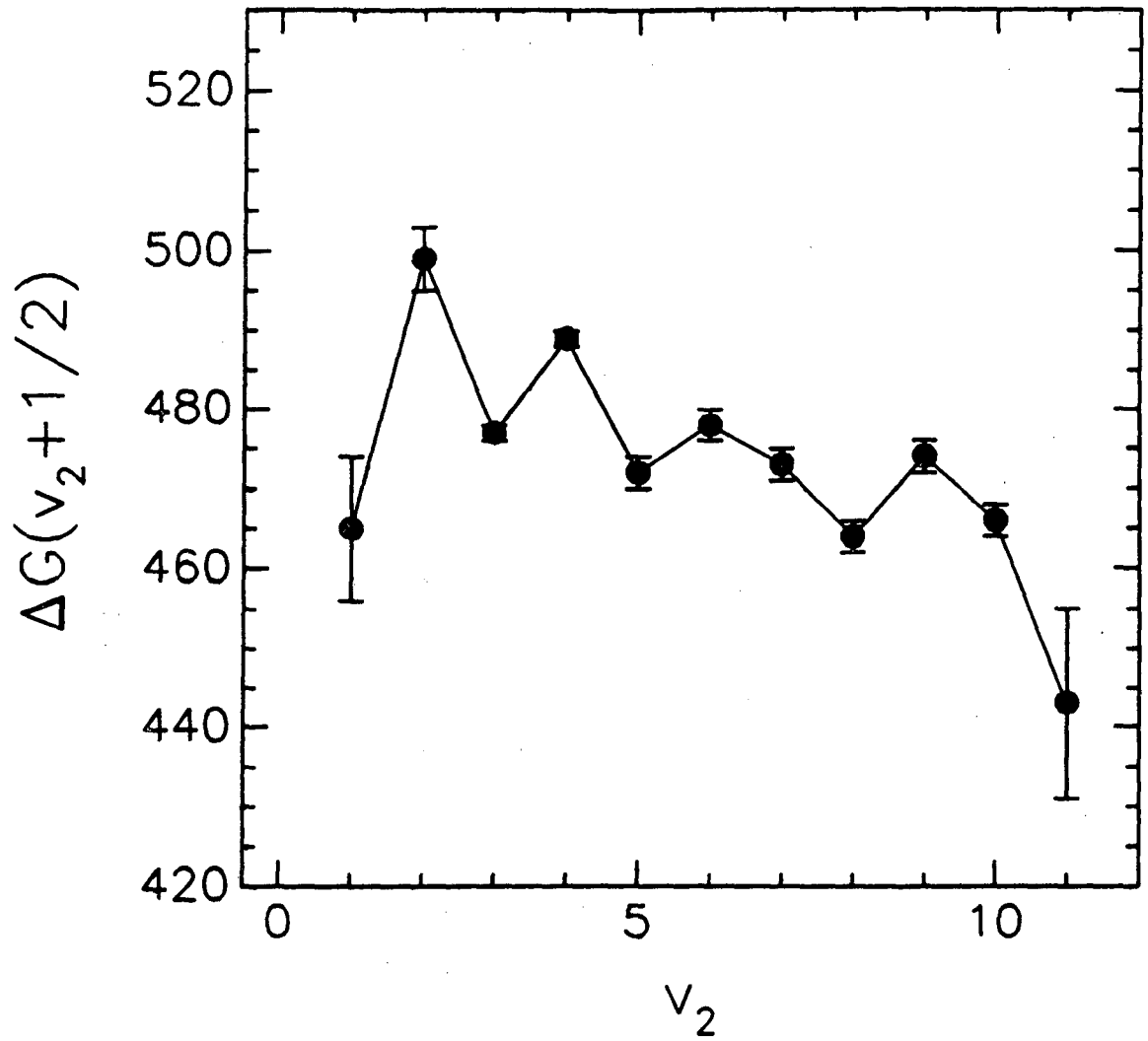
XBL 8611-4770

Fig. 3



XBL 8611-4771

Fig. 4



XBL 8611-4772

Fig. 5



This report was done with support from the Department of Energy. Any conclusions or opinions expressed in this report represent solely those of the author(s) and not necessarily those of The Regents of the University of California, the Lawrence Berkeley Laboratory or the Department of Energy.

Reference to a company or product name does not imply approval or recommendation of the product by the University of California or the U.S. Department of Energy to the exclusion of others that may be suitable.

*LAWRENCE BERKELEY LABORATORY  
TECHNICAL INFORMATION DEPARTMENT  
UNIVERSITY OF CALIFORNIA  
BERKELEY, CALIFORNIA 94720*